

S-Palmitoylation of Junctional Adhesion Molecule C Regulates Its Tight Junction Localization and Cell Migration^{*[5]}

Received for publication, July 26, 2016, and in revised form, February 10, 2017. Published, JBC Papers in Press, February 14, 2017, DOI 10.1074/jbc.M116.730523

Pornpun Aramsangtienchai¹, Nicole A. Spiegelman, Ji Cao, and  Hening Lin²

From the Howard Hughes Medical Institute, Department of Chemistry and Chemical Biology, Cornell University, Ithaca, New York 14853

Edited by Alex Tokier

Junctional adhesion molecule C (JAM-C) is an immunoglobulin superfamily protein expressed in epithelial cells, endothelial cells, and leukocytes. JAM-C has been implicated in leukocyte transendothelial migration, angiogenesis, cell adhesion, cell polarity, spermatogenesis, and metastasis. Here, we show that JAM-C undergoes S-palmitoylation on two juxtamembrane cysteine residues, Cys-264 and Cys-265. We have identified DHHC7 as a JAM-C palmitoylating enzyme by screening all known palmitoyltransferases (DHHCs). Ectopic expression of DHHC7, but not a DHHC7 catalytic mutant, enhances JAM-C S-palmitoylation. Moreover, DHHC7 knockdown decreases the S-palmitoylation level of JAM-C. Palmitoylation of JAM-C promotes its localization to tight junctions and inhibits transwell migration of A549 lung cancer cells. These results suggest that S-palmitoylation of JAM-C can be potentially targeted to control cancer metastasis.

Junctional adhesion molecule C (JAM-C)³ is a member of the JAM family and is localized at the cell-cell contact sites, in particular the tight junction (TJ) region of endothelial and epithelial cells (1–3). JAM-C is a type I transmembrane protein with two conserved immunoglobulin-like domains in the extracellular amino (N)-terminal region (Fig. 1A). At its intracellular carboxyl (C)-terminal region, JAM-C contains a PDZ-binding domain motif, which allows JAM-C to interact with other PDZ motif-containing proteins at the TJ, including ZO-1 and PAR-3 (1–3).

JAM-C has been found to regulate leukocyte adhesion and transmigration across endothelial cells through a heterophilic interaction between endothelial JAM-C and leukocyte integrin MAC-1 ($\alpha M\beta 2$) (4). JAM-C is essential for polarized round spermatids, and JAM-C-deficient mice have defective spermatid differentiation (5). JAM-C deletion in mice leads to neurop-

athy, and some Jam-C mutations affect the integrity of the vascular system and brain (6, 7).

Recently, JAM-C has been shown to play a role in metastasis and development of certain cancer cells (8–11). In melanoma cells, the homophilic JAM-C/JAM-C trans-interaction between melanoma cells and endothelial cells promotes metastasis (12). Additionally, the JAM-C expression level in fibrosarcoma and lung cancer cells is reported to be positively correlated to metastasis. Knocking down JAM-C in highly metastatic lung cancer cells leads to a decrease in cell migration (8, 13). JAM-C, therefore, could be a therapeutic target for certain cancers.

Cys palmitoylation (S-palmitoylation), a reversible lipid post-translational modification, is the addition of a 16-carbon palmitoyl group onto cysteine residues of proteins via a labile thioester bond. S-Palmitoylation plays a crucial role in cell signaling, localization, and protein-protein interactions (14, 15). Palmitoyltransferases (DHHCs) catalyze S-palmitoylation. To date, 23 mammalian DHHCs have been identified (16, 17). Here we showed that JAM-C undergoes S-palmitoylation on two membrane-proximal cysteine residues (Cys-264 and Cys-265), and this modification can be catalyzed by DHHC7. We found that S-palmitoylation of JAM-C promotes its localization to the cell-cell contact region and regulates cell migration.

Results

JAM-C Is S-Palmitoylated on Two Conserved Juxtamembrane Cysteine Residues, Cys-264 and Cys-265—In addition to a PDZ-binding domain, the JAM-C intracellular C terminus contains two transmembrane proximal cysteine residues (Fig. 1A). These two cysteine residues are conserved across multiple mammalian species, suggesting these residues may have an important role (Fig. 1B). Moreover, JAM-C has been identified in palmitoyl-protein proteomics studies as a protein that potentially has Cys palmitoylation, but it was not validated (18). To test whether S-palmitoylation occurs on JAM-C, we used a metabolic labeling strategy using an alkyne-tagged palmitic acid analogue (Alk14) (19, 20). Jurkat cells and human umbilical vein endothelial cells were cultured in the presence of Alk14, and endogenous JAM-C was immunoprecipitated and conjugated to BODIPY-azide via click chemistry (Fig. 2A). JAM-C had fluorescent labeling, suggesting that it contains fatty acylation (Fig. 2B). Similar results were obtained from ectopically expressed FLAG-tagged JAM-C in human embryonic kidney 293T (HEK-293T) cells (Fig. 2C and supplemental Fig. S1).

* This work was supported in part by National Institutes of Health Grant GM098596. The authors declare that they have no conflicts of interest with the contents of this article. The content is solely the responsibility of the authors and does not necessarily represent the official views of the National Institutes of Health.

[5] This article contains supplemental Figs. S1–S5.

¹ Supported in part by a fellowship from the Royal Thai government.

² To whom correspondence should be addressed. E-mail: hl379@cornell.edu.

³ The abbreviations used are: JAM, junctional adhesion molecule; TJ, tight junction; DHHC, palmitoyltransferase; Alk14, alkyne14 (palmitic acid analogue); CCSS, C264S/C265S; 3KR, K276R/K283R/K287R; 4KR, K276R/K283R/K287R/K305R.

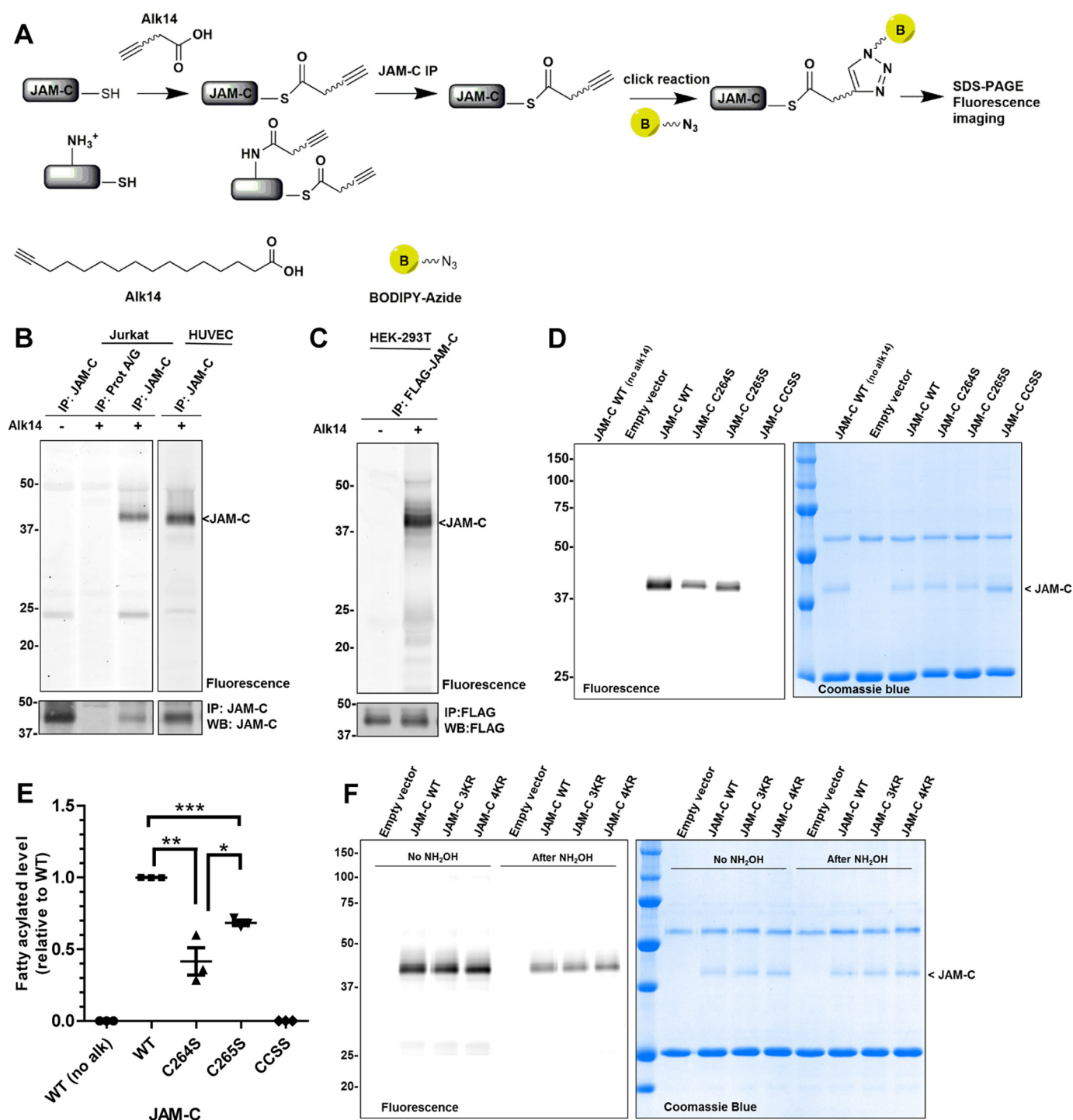
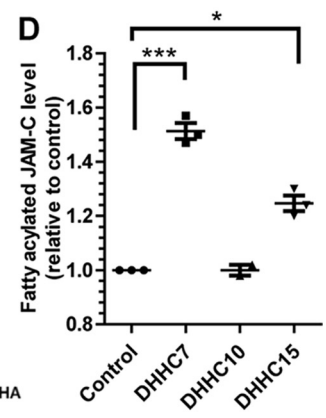
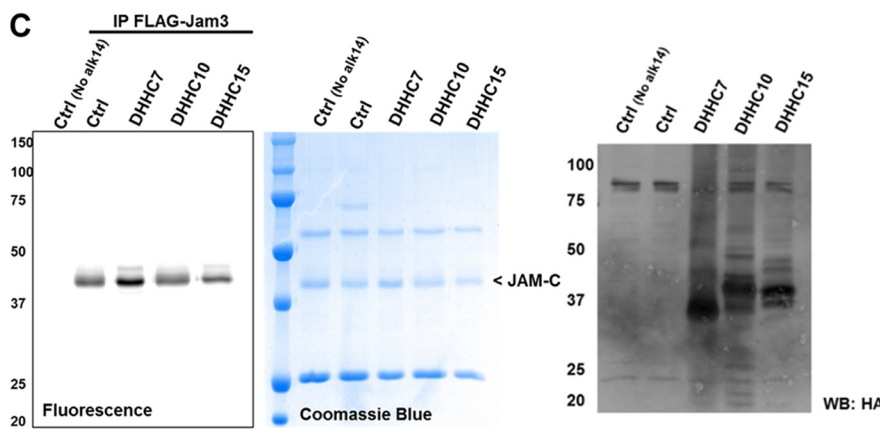
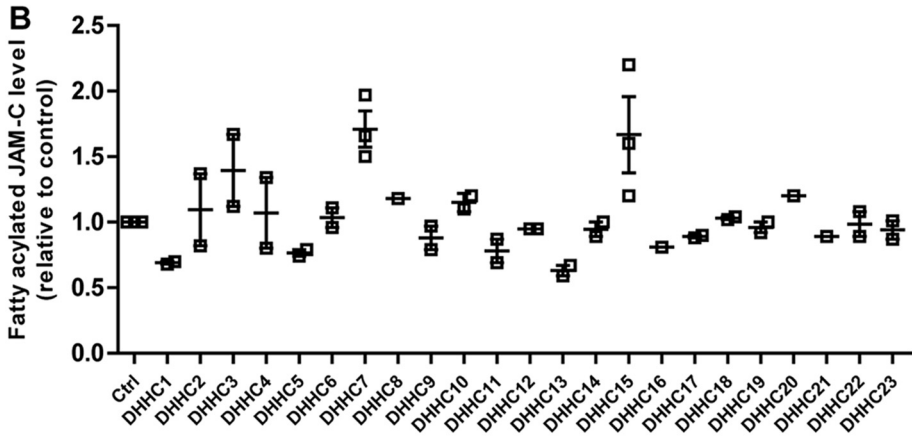
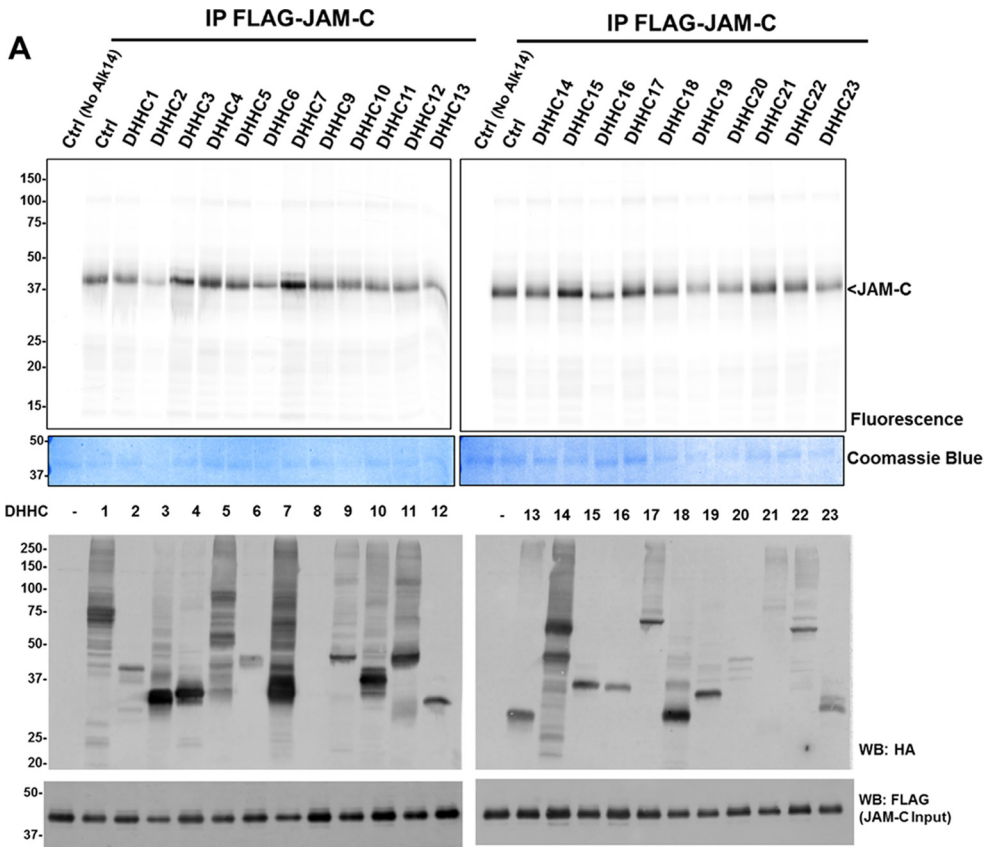


FIGURE 2. S-Palmitoylation of JAM-C depends on Cys-264 and Cys-265. *A*, method for the detection of S-palmitoylation in JAM-C with Alk14, the palmitic acid analogue. Cells were cultured with Alk14 for metabolic labeling. JAM-C was immunoprecipitated from total lysate, and BODIPY-azide was then conjugated to the alkyne group using click chemistry. The fluorescence signal was imaged after SDS-PAGE. *B*, endogenous JAM-C in both Jurkat and human umbilical vein endothelial cells (HUVEC) was labeled by Alk14. *C*, overexpressed FLAG-tagged JAM-C in HEK-293T cells also contained fatty acylation. *D*, the C264S and C265S mutations of JAM-C decreased the Alk14 labeling signal. Compared with the wild type JAM-C, palmitoylation in the single cysteine mutants (C264S and C265S) was reduced, whereas it was abolished in the double cysteine mutant (CCSS). *E*, quantified fatty acylation level of the JAM-C mutants relative to WT ($n = 3$; error bars represent S.D.). The palmitoylation signal was quantified and normalized by the protein level on the Coomassie Blue gel using Quantity One software. *, $p < 0.05$; **, $p < 0.01$; ***, $p < 0.001$. *F*, the cytosolic lysine to arginine mutants 3KR and 4KR of JAM-C did not significantly reduce the Alk14 labeling signal. Representative results from two independent experiments are shown. IP, immunoprecipitation; WB, Western blotting; alk, Alk14.

decrease in the JAM-C palmitoylation level compared with the control with scrambled shRNA, whereas no significant difference in JAM-C palmitoylation was observed in DHHC12 and DHHC15 knockdown cells. These results demonstrate that

JAM-C is a palmitoylation target of endogenous DHHC7. Based on the BioGPS gene database, the DHHC7 gene expression level in the lung is relatively high compared with other tissues. Thus, we also looked at JAM-C palmitoylation in

JAM-C Palmitoylation



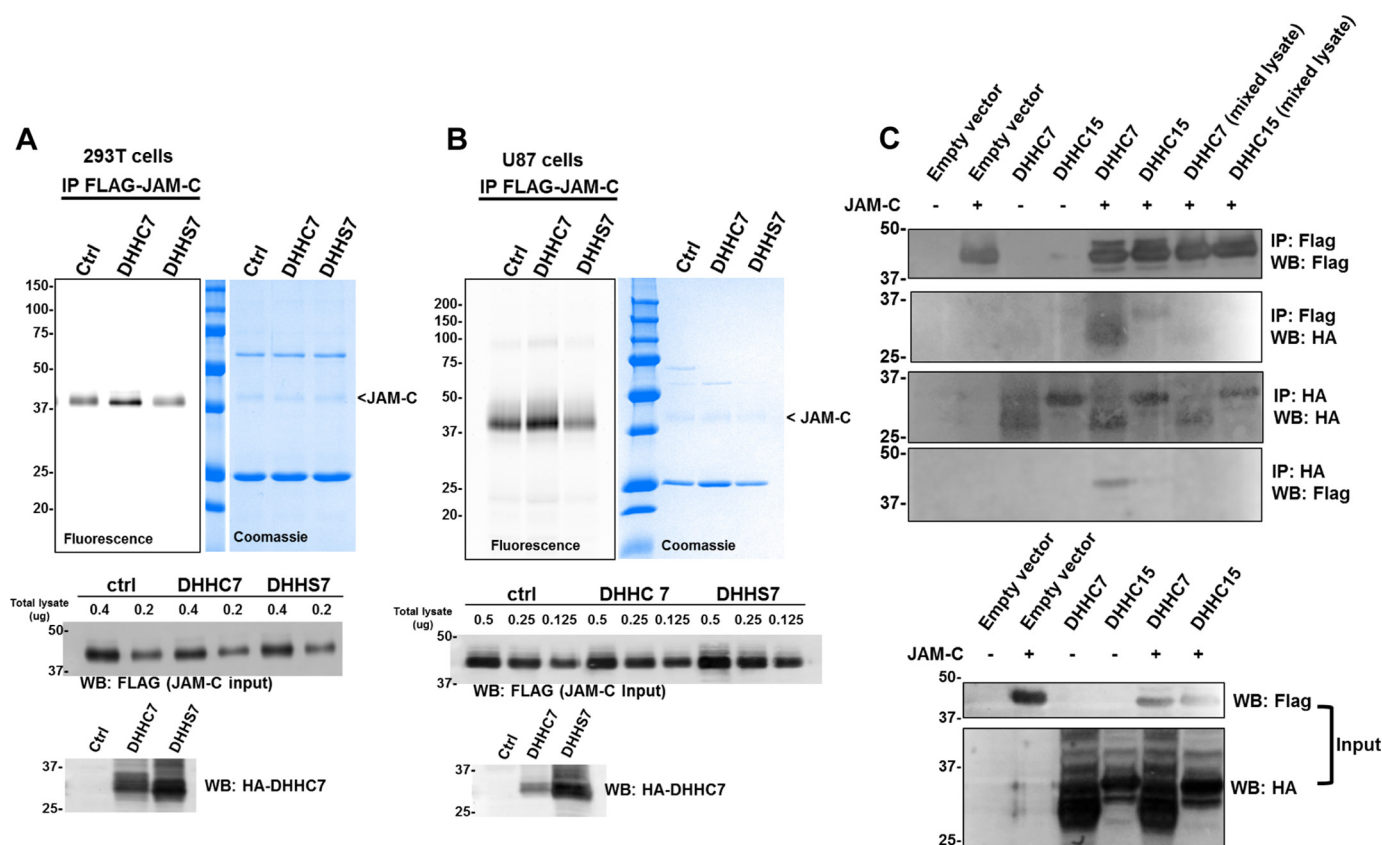


FIGURE 4. DHH7 interacts with JAM-C, and its catalytic activity is required for JAM-C S-palmitoylation. A, overexpression of DHH7, but not DHH57, increased JAM-C S-palmitoylation in HEK-293T cells. HA-tagged DHH7 or HA-tagged DHH57 was co-overexpressed with FLAG-tagged JAM-C. FLAG-tagged JAM-C was pulled down for palmitoylation detection. B, the same experiment as in A was performed in U87 cells. The full FLAG JAM-C input Western blot can be found in supplemental Fig. S5. C, DHH7 interacts with JAM-C. HA-tagged DHH7 was co-overexpressed with FLAG-tagged JAM-C in HEK-293T cells. HA-tagged DHH7 was pulled down, and FLAG-tagged JAM-C was detected by Western blotting and vice versa. In the two lanes labeled with *mixed lysate*, JAM-C and DHH7 or DHH15 were expressed in different cells, and then the cell lysate was mixed before IP. A representative result from two independent experiments is shown. IP, immunoprecipitation; WB, Western blotting; Ctrl, control.

A549 lung cancer cells. DHH7 stable knockdown in A549 cells decreased JAM-C palmitoylation (Fig. 5, D and E).

S-Palmitoylation Promotes JAM-C Localization to the TJ—To further understand the physiological function of JAM-C S-palmitoylation, we investigated whether this modification is required for the TJ localization of JAM-C. FLAG-tagged JAM-C WT and the palmitoylation-deficient CCSS mutant were ectopically expressed in A549 lung cancer cells. The cells were stained with anti-FLAG and anti-ZO-1 antibodies to visualize JAM-C and the TJ, respectively. Images were viewed and analyzed using ZEN 2012 imaging software (Zeiss). Both WT and the CCSS mutant were localized on plasma membrane or intracellular organelles. However, JAM-C WT was more concentrated at the TJ (*white arrow*) as indicated by the co-localization with ZO-1, whereas the CCSS mutant had very little co-localization with ZO-1 (Fig. 6). The co-localization between JAM-C and ZO-1 was quantified using the Coloc2 plug-in in Fiji software and is presented as the mean of Manders' coefficient

(M1 and M2) \pm S.D. Thus, S-palmitoylation of JAM-C facilitates its localization to the TJ.

JAM-C S-Palmitoylation Affects Cell Migration—Because JAM-C S-palmitoylation affects its localization to the cell-cell contact TJ regions, we wondered whether it would also affect cell-cell adhesion. We therefore decided to check whether JAM-C S-palmitoylation could affect cell migration, which is influenced by cell-cell adhesion. A549 cells were transfected with FLAG-tagged JAM-C WT or the CCSS mutant for 24 h. We used a transwell migration assay, which was performed in a 24-well Transwell plate with 8- μ m polycarbonate sterile membranes. Overexpression of JAM-C WT dramatically decreased cell migration compared with control cells that were transfected with an empty vector. In contrast, overexpression of the non-palmitoylatable CCSS mutant only slightly decreased the cell migration compared with control cells that were transfected with an empty vector (Fig. 7, A and B). The difference in cell migration was not due to the variation of cell proliferation

FIGURE 3. DHH7 overexpression enhances the palmitoylation of JAM-C. A, the palmitoylation levels of FLAG-tagged JAM-C co-overexpressed with different HA-tagged DHH1–23 in HEK-293T cells. B, quantification of the results shown in A (mean \pm S.D., $n = 2$). The palmitoylation signal was quantified and normalized with the protein levels on the Coomassie Blue gel using Quantity One software. The signal in control cells without DHH7 overexpression was set to 1.00 and served as the reference point for all other samples. C, DHH7 overexpression most significantly increased JAM-C palmitoylation. A representative result from two independent experiments is shown. D, the quantified fatty acylation level of JAM-C co-overexpressed with DHH7, DHH10, or DHH15 relative to control ($n = 2$; error bars represent S.D.). *, $p < 0.05$; ***, $p < 0.001$. IP, immunoprecipitation; WB, Western blotting; Ctrl, control.

JAM-C Palmitoylation

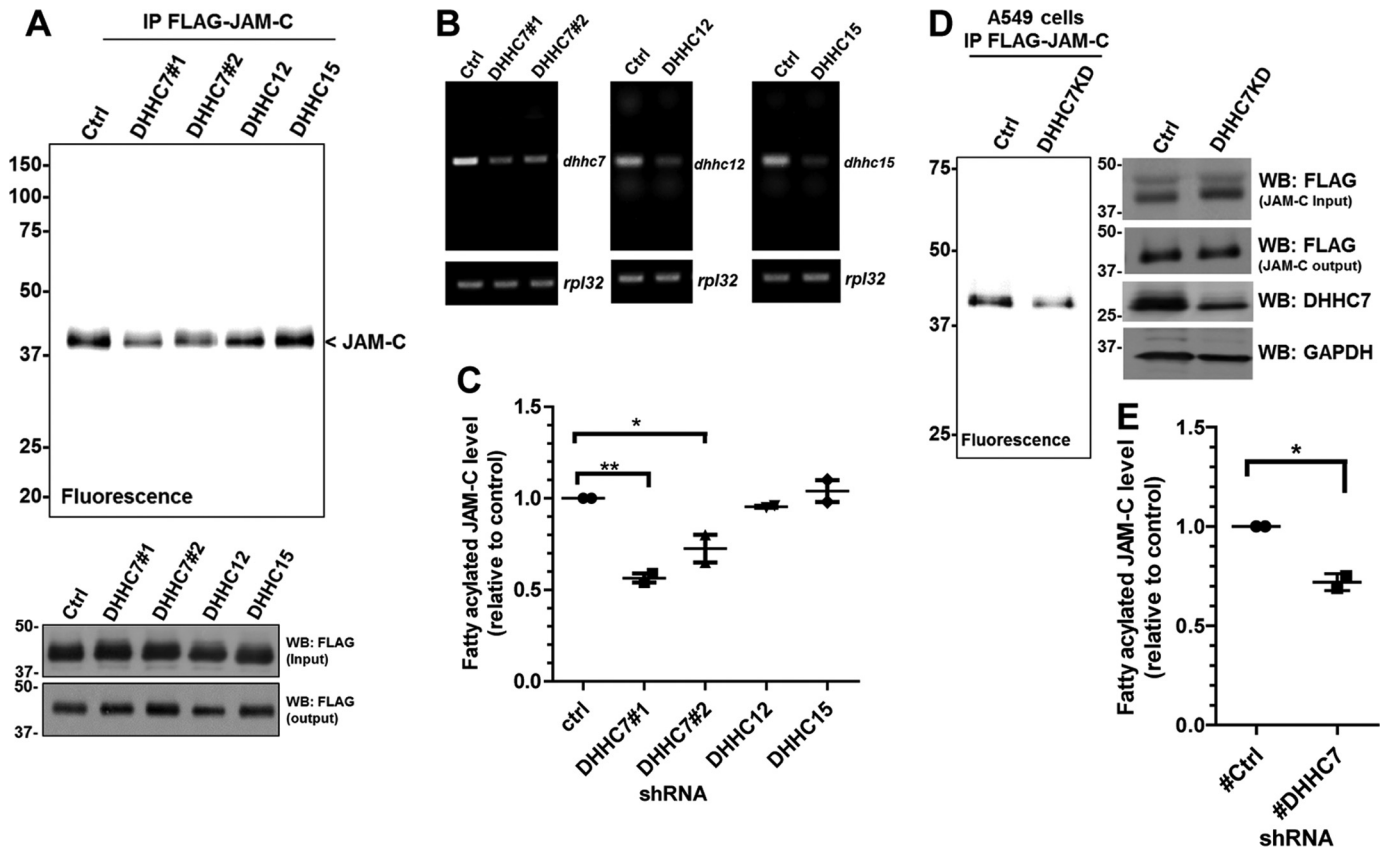


FIGURE 5. JAM-C palmitoylation level decreases in DHHC7 knockdown cells. *A*, HEK-293T cells were infected with lentiviruses containing scrambled shRNA (control) or DHHC7, DHHC12, or DHHC15 shRNAs. Puromycin-resistant cells were selected for stable DHHC knockdown cells and used for FLAG-tagged JAM-C overexpression. The FLAG-tagged JAM-C in the DHHC knockdown cells was then immunoprecipitated and detected for palmitoylation levels by fluorescence labeling. *B*, semiquantitative RT-PCR showing the mRNA levels of *Dhhc7*, *Dhhc12*, and *Dhhc15* in the stable knockdown HEK-293T cells. *C*, quantified fatty acylation levels of FLAG-tagged JAM-C expressed in DHHC7, DHHC12, and DHHC15 knockdown HEK-293T cells relative to control (mean \pm S.D., $n = 2$). The palmitoylation level from each group was quantified and normalized with the corresponding protein level on the Coomassie Blue gel using Quantity One software. The signal from FLAG-tagged JAM-C in the control knockdown cells was set to 1.00 and served as the reference point for the other samples. *D*, DHHC7 knockdown in A549 cells also decreased the palmitoylation of JAM-C. The experiments were carried out similar to that described in *A*. *E*, quantified fatty acylation levels of JAM-C in A549 cells ($n = 2$; error bars represent S.D.). *, $p < 0.05$; **, $p < 0.01$. IP, immunoprecipitation; WB, Western blotting; Ctrl, control.

as there was no significant difference in cell proliferation when JAM-C WT and the CCSS mutant were overexpressed (data not shown). Thus, *S*-palmitoylation of JAM-C affects cell migration.

Discussion

Protein lipidation has become a more widely identified class of protein post-translational modifications and has been found to be involved in numerous biological pathways (15, 24). Here, using a bio-orthogonal palmitic acid probe (19, 20), we demonstrated that both endogenous and ectopically expressed JAM-C contain *S*-palmitoylation. *S*-Palmitoylation occurs on Cys-264 and Cys-265 of JAM-C. The *S*-palmitoylation on JAM-C is relatively resistant to hydroxylamine treatment for which the reason remains unclear. Because the hydroxylamine cleavage depends on the environment (25), one plausible explanation is the *S*-palmitoylation in the membrane-proximal region of JAM-C may be shielded from hydroxylamine attack. However, the decrease in labeling after hydroxylamine treatment supports that JAM-C has *S*-palmitoylation, which is further supported by mutagenesis studies.

The palmitoyltransferase family members share a conserved Asp-His-His-Cys (DHHC)-cysteine-rich domain as a

catalytic domain of the enzyme (26, 27). DHHCs have broad substrate specificity, and how substrate specificity is determined remains unclear. By screening the 23 DHHCs, we have found that overexpression of DHHC7 can substantially increase the JAM-C palmitoylation level. Moreover, we showed that knockdown of DHHC7 decreased the *S*-palmitoyl level of JAM-C, supporting that JAM-C is a direct palmitoylation target of endogenous DHHC7. Nevertheless, other DHHCs may also be able to regulate JAM-C palmitoylation as some DHHCs have redundant functions and act on the same targets (28).

JAM-C has previously been shown to be phosphorylated at Ser-281, and JAM-C localization at the cell-cell contact region is negatively regulated by Ser-281 phosphorylation (29, 30). The JAM-C S281A mutant led to mislocalization and diffusion from the cell-cell contact region. In our case, we observed that JAM-C WT was concentrated at the cell-cell contact region, whereas the CCSS mutant was distributed more evenly on the cell membrane and in the cytosol, which is similar to the effect of S281A. It is therefore possible that there is cross-talk between the phosphorylation and *S*-palmitoylation of JAM-C. However, we found that the non-phosphorylatable JAM-C mutant (S281A) and the phosphomimetic JAM-C mutants (S281D and S281E) had no significant effect on the *S*-palmitoy-

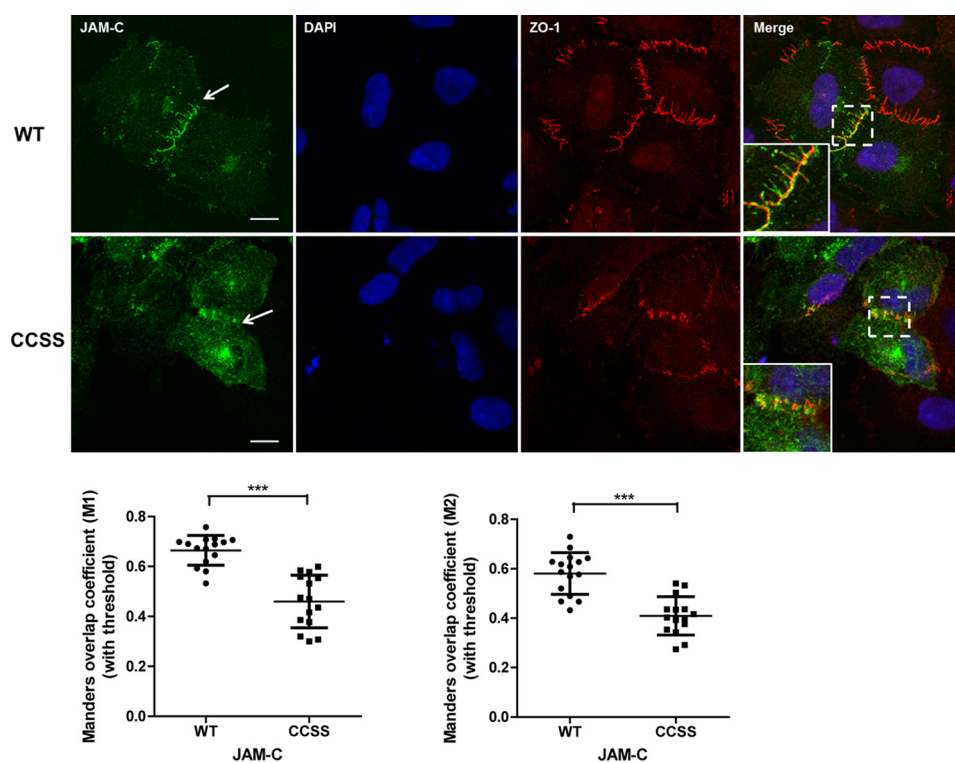


FIGURE 6. S-Palmitoylation promotes JAM-C localization to the tight junction. *Top*, FLAG-tagged JAM-C WT and the CCSS mutant were ectopically expressed in A549 cells. The cells were immunofluorescently stained with anti-FLAG and anti-ZO-1 antibodies after fixation. JAM-C WT was more co-localized with ZO-1 at the tight junction (white arrows), whereas the CCSS mutant had much less co-localization with ZO-1. The cells were visualized at room temperature with a Zeiss LSM 710 confocal microscope with a 63 \times /1.4 oil immersion objective. Images were viewed and analyzed using ZEN 2012 imaging software. These representative images were from three independent experiments with at least 15 FLAG-JAM-C-containing cells analyzed in each experiment. *Scale bars*, 10 μ m. *Bottom*, the co-localization between JAM-C and ZO-1 was analyzed by the Coloc2 plug-in in Fiji software and is presented as the mean of Manders' coefficient ($n = 15$; error bars represent S.D.). ***, $p \leq 0.0001$, Student's t test.

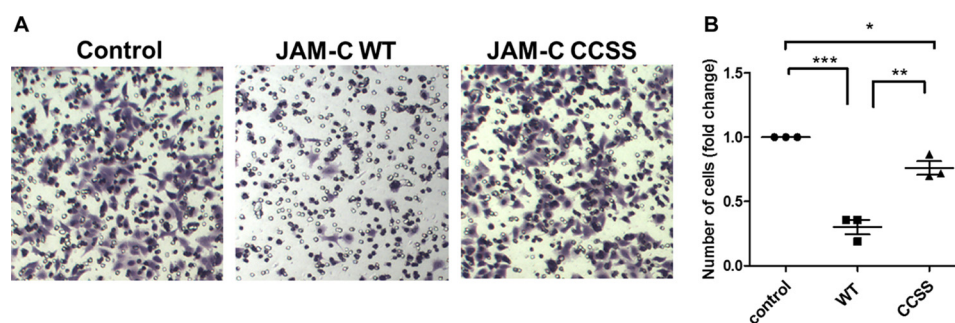


FIGURE 7. JAM-C S-palmitoylation affects cell migration. A549 cells were transfected with FLAG-tagged JAM-C WT or the CCSS mutant for 24 h and then cultured in RPMI 1640 serum-free medium for 14 h. The cell migration assay was then performed in a 24-well Transwell plate with 8- μ m polycarbonate sterile membranes. A total of 3.5×10^4 cells in 200 μ l of RPMI 1640 serum-free medium were plated into each upper chamber and placed in wells containing 600 μ l of RPMI 1640 medium supplemented with 10% FBS. After 24 h, cells on the upper surface were detached with a cotton swab. The chambers were fixed, and cells in the lower filter were stained with 0.1% crystal violet for 15 min and counted. The quantified results were calculated by counting three random fields of migrated cells. The control cells were transfected with an empty pCMV4a vector. *A*, representative images of migrated cells from three independent experiments are shown. *B*, the number of migrated cells per field was quantified and normalized by the value of the control ($n = 3$; error bars represent S.D.). *, $p < 0.05$; **, $p < 0.01$; ***, $p < 0.001$.

lation of JAM-C (supplemental Fig. S4). We could not determine whether the CCSS JAM-C mutant can affect the phosphorylation on JAM-C due to the lack of proper antibodies to detect Ser-281 phosphorylation.

JAM-C has been reported to have homophilic interactions with JAM-C and heterophilic interactions with other PDZ domain-containing proteins such as ZO-1 and PAR3 at the cell tight junction. A possible explanation for the effect of palmitoylation on JAM-C localization is that S-palmitoylation facilitates the interaction of JAM-C with its interacting partners, leading to the enrichment of JAM-C at the cell-cell contact regions.

We demonstrated for the first time that JAM-C palmitoylation can affect cell migration. Overexpression of WT JAM-C decreased migration of A549 cells, but overexpression of the non-palmitoylatable JAM-C mutant did not affect the migration much. S-Palmitoylation of CD44, an adhesion protein, has previously been found to decrease the migration of breast cancer cells, and the invasiveness of cancer is negatively correlated with palmitoylation status of CD44 (31). This is similar to our finding that WT JAM-C decreases the cell migration of A549 cells, but the non-palmitoylatable mutant did not. The effect of JAM-C palmitoylation on cell migration is likely connected to

JAM-C Palmitoylation

its effect on the cell-cell contact localization of JAM-C and cell tight junction integrity. However, exactly how JAM-C palmitoylation regulates cell migration remains elusive.

Currently, only a few substrate proteins for DHHC7 are known, including Fas (32), sex steroid receptors (33), phosphatidylinositol 4-kinase II α (34), G α (35), stress-regulated exon (28) and Scribble (36). Our findings expand the substrate scope of DHHC7, which eventually will help to understand the substrate specificity and function of different DHHCs.

Interestingly, a decrease in DHHC7 levels has been related to tumorigenesis (37), suggesting that DHHC7 may play a role in preventing tumorigenesis. Our findings that JAM-C palmitoylation affects cancer cell migration and that DHHC7 directly controls the palmitoylation level of JAM-C suggest that pharmacologically controlling DHHC7 could be a useful strategy to control cancer cell migration and possibly cancer metastasis. However, to fully take advantage of this, a more detailed understanding of the function of DHHC7 is needed.

Experimental Procedures

JAM-C Cloning and Expression—Human JAM-C cDNA was purchased from Transomic (clone ID BC012147). The full-length cDNA was PCR-amplified by Platinum[®] Pfx DNA polymerase (ThermoFisher) and subcloned into the pCMV-tag 4a vector using the BamHI and EcoRV restriction sites using the following primers: sense, 5'-AGTCAGGGATCCATGGCGCTGAGGCGGCCA-3'; antisense, 5'-AGTCAGGATATC-GATCAAAACGATGACTTGTGTCT-3'. JAM-C mutants (C264S, C265S, and CCSS) were generated by QuikChange mutagenesis. The JAM-C in pCMV-tag 4a vector was PCR-amplified using Phusion[®] high fidelity DNA polymerase and the following mutagenic primers (the underlined nucleotide sequences code for the mutated amino acid): C264S: sense, 5'-CCCTGATCACGTTGGGCATCAGCTGTGCATACAG-ACGTGGCTA-3'; antisense, 5'-GATGCCCAACGTGATC-AGGG-3'; C265S: sense, 5'-TGATCACGTTGGGCAT-CTGCAGTGCATACAGACGTGGCTACTT-3'; antisense, 5'-GCAGATGCCCAACGTGATCA-3'; and CCSS: sense, 5'-CCCTGATCACGTTGGGCATCAGCAGTGCATACAG-ACGTGGCTACTT-3'; antisense, 5'-GATGCCCAACGTG-ATCAGGG-3'. The plasmids of DHHC1–23 in pEF-BOS-HA vector for screening were generously provided by Prof. Maurine Linder and Prof. Masaki Fukata.

Cell Culture and Transfection—HEK-293T cells were cultured in Dulbecco's modified Eagle's medium (DMEM) supplemented with 10% fetal bovine serum (Invitrogen), and Jurkat and A549 cells were cultured in Roswell Park Memorial Institute (RPMI) 1640 medium (Invitrogen) supplemented with 10% fetal bovine serum (Invitrogen). All cells were incubated in a humidified incubator at 37 °C with 5% CO₂. FuGENE[®] 6 transfection reagent (Promega) was used for cell transfection according to the manufacturer's instruction.

Antibodies—Anti-FLAG[®] M2-peroxidase (HRP) antibody (mouse monoclonal IgG) for Western blotting and anti-FLAG M2 affinity gel for immunoprecipitation were purchased from Sigma (catalogue numbers A8592 and A2220, respectively). Anti-FLAG antibody (mouse monoclonal IgG1) for immunofluorescence was purchased from Cell Signaling Technology

(catalogue number 8146). Secondary antibody Alexa Fluor[®] 488 conjugate (mouse polyclonal IgG) was purchased from ThermoFisher (catalogue number A-11001). Anti-HA-peroxidase (rat IgG1) was purchased from Roche Applied Science (catalogue number 12013819001). The anti-human JAM-C antibody (mouse monoclonal IgG) was purchased from Enzo Life Sciences (catalogue number ALX-803-306), and anti-DHHC7 (rabbit IgG) antibody was purchased from Assay-Biotech (catalogue number R12-3691). All other peroxidase-conjugated secondary antibodies were from Santa Cruz Biotechnology.

Western Blotting—Cells were collected and lysed with 1% Nonidet P-40 lysis buffer (50 mM Tris-HCl (pH 7.4), 150 mM NaCl, and 1% (v/v) Nonidet P-40 (Igepal) containing protease inhibitor mixtures (Sigma)). Protein concentration was determined by Bradford assay (Pierce[™] Coomassie Protein Assay kit). Protein samples were separated by 12% SDS-PAGE and transferred to PVDF membrane (Bio-Rad) for 90 min. The membrane was blocked with 5% bovine serum albumin (BSA; Santa Cruz Biotechnology) in TBST (25 mM Tris-HCl (pH 7.4), 150 mM NaCl, and 0.1% Tween 20) and incubated with the primary antibody for 3 h at room temperature or overnight at 4 °C. After washing five times with TBST, the membrane was incubated with the secondary antibody for 1 h at room temperature. The membrane was washed five more times with TBST before it was developed in ECL-Plus Western blotting detection reagent (GE Healthcare). The signal was visualized using a Typhoon 9400 variable mode imager (GE Healthcare) with 457-nm excitation and 526-nm detection filters using a photomultiplier tube setting of 600 V (normal sensitivity). The signal was analyzed by ImageQuant TL v2005 and Quantity One (Bio-Rad).

Metabolic Labeling of Palmitoylation on FLAG-tagged JAM-C—Cells were transfected with FLAG-JAM-C in pCMV4a vector. After 24 h, the cells were incubated with 50 μ M Alk14 in medium supplemented with 10% FBS for 6 h. Cells were collected and washed with 1 \times phosphate-buffered saline (PBS) three times. The cell pellets were lysed with 1% Nonidet P-40 lysis buffer. The protein concentration was determined by Bradford assay (Pierce Coomassie Protein Assay kit). The expression level of FLAG-JAM-C was confirmed by Western blotting. For FLAG-JAM-C immunoprecipitation, 25 μ l of anti-FLAG M2 affinity gel was added into 600 μ g of total cell lysate with a final volume of 1 ml in an Eppendorf tube. The samples were gently agitated at 4 °C for 2 h. The samples were then centrifuged at 1,000 \times g for 2 min at 4 °C to remove the supernatant. The beads were washed three times with 0.1% Nonidet P-40 lysis buffer. After the last wash, all the buffer was removed. The beads were resuspended in 15 μ l of 0.1% Nonidet P-40 buffer. To perform the click reaction, 5.6 μ l of the reaction master mixture was added to each sample. The click reaction master mixture contains the following: 3 μ l of 1 mM BODIPY-azide in *N,N*-dimethylformamide, 1 μ l of 50 mM tris(2-carboxyethyl)phosphine hydrochloride (Calbiochem) in water, 0.6 μ l of 10 mM tris[(1-benzyl-1*H*-1,2,3-triazol-4-yl)methyl] amine (Sigma) in *N,N*-dimethylformamide, and 1 μ l of 50 mM CuSO₄ in water. After 1 h at room temperature, 20 μ l of 3 \times protein loading buffer (187 mM Tris-HCl (pH 6.8), 6% SDS, 150 mM

DTT, 30% (v/v) glycerol, and 0.006% bromphenol blue) was added to each sample, and the samples were boiled at 95 °C for 5 min and centrifuged at $17,000 \times g$ for 2 min. The supernatants were transferred into new Eppendorf tubes and loaded for 12% SDS-PAGE. The fluorescence signal was visualized with a Typhoon 9400 variable mode imager using 488-nm excitation and 520-nm detection filters and a photomultiplier tube setting of 550 V (normal sensitivity). The signal was analyzed by ImageQuant TL v2005 and quantified by Quantity One within a linear range of exposure.

Generation of DHHC7, DHHC12, and DHHC15 Stable Knock-down in HEK-293T Cell Line—Different DHHC shRNA lentiviral plasmids in pLKO.1-puro vector were purchased from Sigma (catalogue numbers DHHC7-SHCLNG-NM_017740, shRNA1-TRCN0000143647, shRNA2-TRCN0000275633; DHHC12-SHCLNG-NM_025428; and DHHC15-SHCLNG-NM_144969). To generate the lentiviruses, low passage number HEK-293T cells in a 10-cm^3 plates were transfected with 6 μg of each DHHC shRNA, 4 μg of pCMV-dR8.2, and 2 μg of pM2D.G mixed with 36 μl of FuGENE 6 (Promega). The cell media containing the lentiviruses were collected after 48 h by centrifugation and filtered through 0.45- μm syringe filter to remove cell debris. The day before infection, 3×10^5 cells of low passage number HEK-293T cells were split into each well of a 6-well plate and grown overnight in 2 ml of DMEM with 10% FBS. The media were then removed and replaced with a mixture of 1.5 ml of the lentivirus medium collected above, 0.5 ml of fresh DMEM with 10% FBS, and 6 $\mu\text{g}/\mu\text{l}$ Polybrene (Sigma). After 6 h, 3 ml of DMEM with 10% FBS was added to each well, and after 48 h, 1.5 $\mu\text{g}/\mu\text{l}$ puromycin dihydrochloride (Santa Cruz Biotechnology) was added to the cells to select for stable DHHC knockdown cells.

Cell Migration Assay—A549 cells were transfected with FLAG-JAM-C WT in pCMV4a, the FLAG-tagged CCSS mutant in pCMV4a, or the empty pCMV4a vector (control) for 24 h and then cultured in RPMI 1640 serum-free medium for an additional 14 h. The cell migration assay was performed in a 24-well Transwell plate with 8- μm polycarbonate sterile membrane (Corning Inc.). A total of 3.5×10^4 cells in 200 μl of RPMI 1640 serum-free medium were plated in each upper chamber and then placed in wells containing 600 μl of RPMI 1640 medium supplemented with 10% FBS. After 24 h, the cells on the upper surface were detached with a cotton swab, and the upper chambers were fixed. The cells in the lower filter were stained with 0.1% crystal violet for 15 min and then counted. The quantified results represent three random fields of migrated cells.

Immunofluorescence Microscopy—A total of 2×10^5 A549 cells were split into each glass bottom culture dish (MatTek) and cultured overnight. The cells were then transfected with either the FLAG-JAM-C WT in pCMV4a vector or the CCSS mutant. After 24 h, cells were washed twice with 2 ml of $1 \times$ PBS (ThermoFisher), fixed with 4% paraformaldehyde in PBS on ice for 15 min, and then kept at room temperature for 5 min. Then cells were subsequently washed three times with 2 ml of $1 \times$ PBS and incubated with 0.1% saponin (TCI America) with 3% BSA in $1 \times$ PBS at room temperature. After 1 h, the blocking solution was removed, and the anti-FLAG antibody (rabbit monoclonal

IgG1; 1:1,000; Cell Signaling Technology) and the anti-ZO1 antibody (mouse monoclonal IgG1; 1:800; BD Biosciences) in a saponin-BSA solution were added to the cells and incubated at 4 °C overnight. The cells were washed with 1 ml of saponin-BSA solution five times and then incubated with the secondary antibodies conjugated with Alexa Fluor 488 (goat anti-rabbit IgG polyclonal antibody; ThermoFisher; 1:1,000) or Texas Red[®] (goat anti-mouse IgG polyclonal antibody; ThermoFisher; 1:1,000) in the saponin-BSA solution at room temperature for 1 h. The cells were washed with 1 ml of saponin-BSA solution five times, then mounted with 200 μl of DAPI Fluoromount-G (Southern Biotech), and covered with a cover glass. After 24 h, the cells were visualized with a Zeiss LSM 710 confocal microscope with a 63 \times /1.4 oil immersion objective. Images were viewed and analyzed using ZEN 2012 imaging software. For JAM-C and ZO-1 co-localization analysis, the Manders' overlap coefficient with automatic thresholds (M1 and M2) was calculated using the Coloc2 plug-in in Fiji (background subtraction; rolling ball radius, 50 pixels) (38).

Statistical Analysis—Data are shown as mean \pm S.D. Differences were analyzed by two-tailed Student's *t* test between two groups: *, $p < 0.05$; **, $p < 0.01$; ***, $p < 0.001$.

Author Contributions—P. A. and H. L. designed the experiments and wrote the paper. N. A. S. carried out the experiment shown in Figs. 3, A and B, and 4C, and supplemental Figs. S1–S3 and synthesized Alk14. J. C. performed and analyzed the experiment shown in Fig. 7. All authors reviewed and approved the final version of the manuscript.

Acknowledgment—The imaging data were enabled by the Cornell University Biotechnology Resource Center with National Institutes of Health Grant 1S10RR025502 funding for the Zeiss LSM 710 confocal microscope.

References

1. Ebnet, K., Suzuki, A., Ohno, S., and Vestweber, D. (2004) Junctional adhesion molecules (JAMs): more molecules with dual functions? *J. Cell Sci.* **117**, 19–29
2. Keiper, T., Santoso, S., Nawroth, P. P., Orlova, V., and Chavakis, T. (2005) The role of junctional adhesion molecules in cell-cell interactions. *Histol. Histopathol.* **20**, 197–203
3. Bazzoni, G. (2003) The JAM family of junctional adhesion molecules. *Curr. Opin. Cell Biol.* **15**, 525–530
4. Weber, C., Fraemohs, L., and Dejana, E. (2007) The role of junctional adhesion molecules in vascular inflammation. *Nat. Rev. Immunol.* **7**, 467–477
5. Gliki, G., Ebnet, K., Aurrand-Lions, M., Imhof, B. A., and Adams, R. H. (2004) Spermatid differentiation requires the assembly of a cell polarity complex downstream of junctional adhesion molecule-C. *Nature* **431**, 320–324
6. Guo, J., Wang, L., Zhang, Y., Wu, J., Arpag, S., Hu, B., Imhof, B. A., Tian, X., Carter, B. D., Suter, U., and Li, J. (2014) Abnormal junctions and permeability of myelin in PMP22-deficient nerves. *Ann. Neurol.* **75**, 255–265
7. Akawi, N. A., Canpolat, F. E., White, S. M., Quilis-Esquerria, J., Morales Sanchez, M., Gamundi, M. J., Mochida, G. H., Walsh, C. A., Ali, B. R., and Al-Gazali, L. (2013) Delineation of the clinical, molecular and cellular aspects of novel JAM3 mutations underlying the autosomal recessive hemorrhagic destruction of the brain, subependymal calcification, and congenital cataracts. *Hum. Mutat.* **34**, 498–505

8. Hao, S., Yang, Y., Liu, Y., Yang, S., Wang, G., Xiao, J., and Liu, H. (2014) JAM-C promotes lymphangiogenesis and nodal metastasis in non-small cell lung cancer. *Tumour Biol.* **35**, 5675–5687
9. Leinster, D. A., Colom, B., Whiteford, J. R., Ennis, D. P., Lockley, M., McNeish, I. A., Aurrand-Lions, M., Chavakis, T., Imhof, B. A., Balkwill, F. R., and Nourshargh, S. (2013) Endothelial cell junctional adhesion molecule C plays a key role in the development of tumors in a murine model of ovarian cancer. *FASEB J.* **27**, 4244–4253
10. Arcangeli, M. L., Frontera, V., Bardin, F., Thomassin, J., Chetaille, B., Adams, S., Adams, R. H., and Aurrand-Lions, M. (2012) The junctional adhesion molecule-B regulates JAM-C-dependent melanoma cell metastasis. *FEBS Lett.* **586**, 4046–4051
11. Tenan, M., Aurrand-Lions, M., Widmer, V., Alimenti, A., Burkhardt, K., Lazeyras, F., Belkouch, M. C., Hammel, P., Walker, P. R., Duchosal, M. A., Imhof, B. A., and Dietrich, P. Y. (2010) Cooperative expression of junctional adhesion molecule-C and -B supports growth and invasion of glioma. *Glia* **58**, 524–537
12. Langer, H. F., Orlova, V. V., Xie, C., Kaul, S., Schneider, D., Lonsdorf, A. S., Fahrleitner, M., Choi, E. Y., Dutoit, V., Pellegrini, M., Grossklaus, S., Nawroth, P. P., Baretton, G., Santoso, S., Hwang, S. T., et al. (2011) A novel function of junctional adhesion molecule-C in mediating melanoma cell metastasis. *Cancer Res.* **71**, 4096–4105
13. Fuse, C., Ishida, Y., Hikita, T., Asai, T., and Oku, N. (2007) Junctional adhesion molecule-C promotes metastatic potential of HT1080 human fibrosarcoma. *J. Biol. Chem.* **282**, 8276–8283
14. Smotrys, J. E., and Linder, M. E. (2004) Palmitoylation of intracellular signaling proteins: regulation and function. *Annu. Rev. Biochem.* **73**, 559–587
15. Resh, M. D. (1999) Fatty acylation of proteins: new insights into membrane targeting of myristoylated and palmitoylated proteins. *Biochim. Biophys. Acta* **1451**, 1–16
16. Fukata, M., Fukata, Y., Adesnik, H., Nicoll, R. A., and Brecht, D. S. (2004) Identification of PSD-95 palmitoylating enzymes. *Neuron* **44**, 987–996
17. Linder, M. E., and Jennings, B. C. (2013) Mechanism and function of DHHC S-acyltransferases. *Biochem. Soc. Trans.* **41**, 29–34
18. Kang, R., Wan, J., Arstikaitis, P., Takahashi, H., Huang, K., Bailey, A. O., Thompson, J. X., Roth, A. F., Drisdell, R. C., Mastro, R., Green, W. N., Yates, J. R., 3rd, Davis, N. G., and El-Husseini, A. (2008) Neural palmitoyl-proteomics reveals dynamic synaptic palmitoylation. *Nature* **456**, 904–909
19. Yount, J. S., Zhang, M. M., and Hang, H. C. (2011) Visualization and identification of fatty acylated proteins using chemical reporters. *Curr. Protoc. Chem. Biol.* **3**, 65–79
20. Wilson, J. P., Raghavan, A. S., Yang, Y. Y., Charron, G., and Hang, H. C. (2011) Proteomic analysis of fatty-acylated proteins in mammalian cells with chemical reporters reveals S-acylation of histone H3 variants. *Mol. Cell. Proteomics* **10**, M110.001198
21. Jiang, H., Khan, S., Wang, Y., Charron, G., He, B., Sebastian, C., Du, J., Kim, R., Ge, E., Mostoslavsky, R., Hang, H. C., Hao, Q., and Lin, H. (2013) SIRT6 regulates TNF- α secretion through hydrolysis of long-chain fatty acyl lysine. *Nature* **496**, 110–113
22. Jing, S. Q., and Trowbridge, I. S. (1987) Identification of the intermolecular disulfide bonds of the human transferrin receptor and its lipid-attachment site. *EMBO J.* **6**, 327–331
23. Dietrich, L. E., and Ungerermann, C. (2004) On the mechanism of protein palmitoylation. *EMBO Rep.* **5**, 1053–1057
24. Resh, M. D. (2012) Targeting protein lipidation in disease. *Trends Mol. Med.* **18**, 206–214
25. Iwamoto, M., Sudo, Y., Shimono, K., and Kamo, N. (2001) Selective reaction of hydroxylamine with chromophore during the photocycle of pharionis phorbodopsin. *Biochim. Biophys. Acta* **1514**, 152–158
26. Roth, A. F., Feng, Y., Chen, L., and Davis, N. G. (2002) The yeast DHHC cysteine-rich domain protein Akr1p is a palmitoyl transferase. *J. Cell Biol.* **159**, 23–28
27. Lobo, S., Greentree, W. K., Linder, M. E., and Deschenes, R. J. (2002) Identification of a Ras palmitoyltransferase in *Saccharomyces cerevisiae*. *J. Biol. Chem.* **277**, 41268–41273
28. Tian, L., McClafferty, H., Jeffries, O., and Shipston, M. J. (2010) Multiple palmitoyltransferases are required for palmitoylation-dependent regulation of large conductance calcium- and voltage-activated potassium channels. *J. Biol. Chem.* **285**, 23954–23962
29. Mandicourt, G., Iden, S., Ebnet, K., Aurrand-Lions, M., and Imhof, B. A. (2007) JAM-C regulates tight junctions and integrin-mediated cell adhesion and migration. *J. Biol. Chem.* **282**, 1830–1837
30. Ebnet, K., Aurrand-Lions, M., Kuhn, A., Kiefer, F., Butz, S., Zander, K., Meyer zu Brickwedde, M. K., Suzuki, A., Imhof, B. A., and Vestweber, D. (2003) The junctional adhesion molecule (JAM) family members JAM-2 and JAM-3 associate with the cell polarity protein PAR-3: a possible role for JAMs in endothelial cell polarity. *J. Cell Sci.* **116**, 3879–3891
31. Babina, I. S., McSherry, E. A., Donatello, S., Hill, A. D., and Hopkins, A. M. (2014) A novel mechanism of regulating breast cancer cell migration via palmitoylation-dependent alterations in the lipid raft affiliation of CD44. *Breast Cancer Res.* **16**, R19
32. Rossin, A., Durivault, J., Chakhtoura-Feghali, T., Lounnas, N., Gagnoux-Palacios, L., and Hueber, A. O. (2015) Fas palmitoylation by the palmitoyl acyltransferase DHHC7 regulates Fas stability. *Cell Death Differ.* **22**, 643–653
33. Pedram, A., Razandi, M., Deschenes, R. J., and Levin, E. R. (2012) DHHC-7 and -21 are palmitoylacyltransferases for sex steroid receptors. *Mol. Biol. Cell* **23**, 188–199
34. Lu, D., Sun, H. Q., Wang, H., Barylko, B., Fukata, Y., Fukata, M., Albanesi, J. P., and Yin, H. L. (2012) Phosphatidylinositol 4-kinase II α is palmitoylated by Golgi-localized palmitoyltransferases in cholesterol-dependent manner. *J. Biol. Chem.* **287**, 21856–21865
35. Tsutsumi, R., Fukata, Y., Noritake, J., Iwanaga, T., Perez, F., and Fukata, M. (2009) Identification of G protein α subunit-palmitoylating enzyme. *Mol. Cell. Biol.* **29**, 435–447
36. Chen, B., Zheng, B., DeRan, M., Jarugumilli, G. K., Fu, J., Brooks, Y. S., and Wu, X. (2016) ZDHHC7-mediated S-palmitoylation of Scribble regulates cell polarity. *Nat. Chem. Biol.* **12**, 686–693
37. Gaspar, C., Cardoso, J., Franken, P., Molenaar, L., Morreau, H., Möslein, G., Sampson, J., Boer, J. M., de Menezes, R. X., and Fodde, R. (2008) Cross-species comparison of human and mouse intestinal polyps reveals conserved mechanisms in adenomatous polyposis coli (APC)-driven tumorigenesis. *Am. J. Pathol.* **172**, 1363–1380
38. Schindelin, J., Arganda-Carreras, I., Frise, E., Kaynig, V., Longair, M., Pietzsch, T., Preibisch, S., Rueden, C., Saalfeld, S., Schmid, B., Tinevez, J. Y., White, D. J., Hartenstein, V., Eliceiri, K., Tomancak, P., et al. (2012) Fiji: an open-source platform for biological-image analysis. *Nat. Methods* **9**, 676–682

S-Palmitoylation of Junctional Adhesion Molecule C Regulates Its Tight Junction Localization and Cell Migration

Pornpun Aramsangtienchai, Nicole A. Spiegelman, Ji Cao and Hening Lin

J. Biol. Chem. 2017, 292:5325-5334.

doi: 10.1074/jbc.M116.730523 originally published online February 14, 2017

Access the most updated version of this article at doi: [10.1074/jbc.M116.730523](https://doi.org/10.1074/jbc.M116.730523)

Alerts:

- [When this article is cited](#)
- [When a correction for this article is posted](#)

[Click here](#) to choose from all of JBC's e-mail alerts

Supplemental material:

<http://www.jbc.org/content/suppl/2017/02/14/M116.730523.DC1>

This article cites 38 references, 14 of which can be accessed free at

<http://www.jbc.org/content/292/13/5325.full.html#ref-list-1>